PHYSICAL REVIEW E **80**, 060301(R) (2009)

Sliding through a superlight granular medium

F. Pacheco-Vázquez[1] and J. C. Ruiz-Suárez[2,*]

[1]*Departamento de Física Aplicada, CINVESTAV-Mérida, Mérida, Yucatán 97310, Mexico*

[2]*CINVESTAV-Monterrey, PIIT Autopista Nueva al Aeropuerto Km. 9.5, Apodaca, Nuevo León 66600, Mexico*

(Received 27 February 2009; revised manuscript received 23 October 2009; published 14 December 2009)

We explore the penetration dynamics of an intruder in a granular medium composed of expanded polystyrene spherical particles. Three features distinguish our experiment from others studied so far in granular physics: (a) the impact is horizontal, decoupling the effects of gravity and the drag force; (b) the density of the intruder ρ_i is up to 350 times larger than the density of the granular medium ρ_m; and (c) the way the intruder moves through the material, sliding at the bottom of the column with small friction. Under these conditions we find that the final penetration D scales with (ρ_i/ρ_m) and the drag force F_d and D saturate with the height of the granular bed.

DOI: 10.1103/PhysRevE.80.060301 PACS number(s): 45.70.Mg

A projectile impacting against a granular medium exemplifies the interesting nature of granular matter. Whether the projectile is an asteroid striking the crust of a planet [1,2] or an object thrown against a granular bed in the laboratory [3–16], once the intruder makes contact with the medium it inevitably encounters a stopping force. It is the character of this force that granular physics aims to understand. Fortunately, although there are still unanswered questions, great progress has been made. It is known, for instance, that the energy of the impact determines the strength of the stopping force [4] and also how the penetration depth scales with the relevant variables of the collision [7,8]. It is known, as well, that the continuous creation and collapse of jammed states, within the trajectory of the intruder, explains the fluctuating essence of the drag force [6,17–19]. If the system is confined, as is normally the situation in experiments carried out in the laboratory, the walls and bottom affect the penetration dynamics [15,16,20]. In the case of intruders pulled through granular systems the drag forces have a linear dependence with depth although nonlinear components have been observed [21]. All in all, the physical picture we have about these phenomena seemed to be reasonably drawn. However, all the previous experiments have been carried out with intruders and granular systems whose densities are of the same order of magnitude. Even in the case of experiments in dry quicksand [9–12], the density contrast between intruders and grains is relatively small.

What would occur with the rheology of a granular medium if, instead of reducing the packing fraction like in dry quicksand, the density of the bed constituents is considerably small? In this Rapid Communication we explore such a case: the penetration dynamics of an intruder in a column composed of expanded polystyrene beads. As far as we know, these beads are much lighter than any other particles of similar size studied in granular physics. We study the horizontal impact of an intruder at the bottom of a granular bed. We measured drag forces and final penetrations and found that both of them saturate as a function of the bed height in a Janssen-like fashion. A third distinctive feature of this experiment is the way the intruder penetrates the medium. Normally, intruders are forced to move in granular materials attached to rods, which perturb the system [21]. In our experiments, the intruder moves by its own inertia sliding with small friction on top of the first monolayer of the column.

Figure 1(a) shows a schematic view of the experimental setup. It consists of a rectangular Plexiglas container whose dimensions are 240 cm (length), 60 cm (height), and 20 cm (wide). The first part of the container is a 110 cm ramp. The ramp is smoothly connected, in its lower part, to the channel that confines the particles. There is a wall at the middle of the container that does not touch the base, leaving a gate where a sliding object can eventually pass through, penetrating the column. The angle the ramp makes with the horizontal base is 17°. The diameter and density of the polystyrene particles are, respectively, 5.0 ± 0.3 mm and 0.014 ± 0.002 g/cm^3. The intruder is a hollow acrylic disk with diameter $d=5.2$ cm and thickness $\tau=1.6$ cm. Its density is varied by putting inside circular lead sheets. The ramp is covered by a monolayer of particles and the channel is filled to a height h [see Fig. 1(a)]. The disk released from rest at a height H sliding downhill mounted on the monolayer, acquires a final velocity V_0 and penetrates the bed and stops at a distance D, where the zero of D is the position at which the

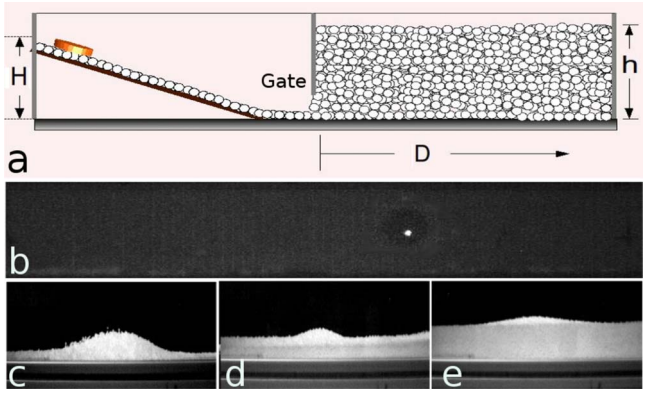

FIG. 1. (Color online) (a) Experimental setup, details are explained in the text. (b) Bottom view, and (c)–(e) lateral views, from which a traveling lump is observed for h equal to 6, 8, and 10 cm.

*Corresponding author. cruiz@mda.cinvestav.mx

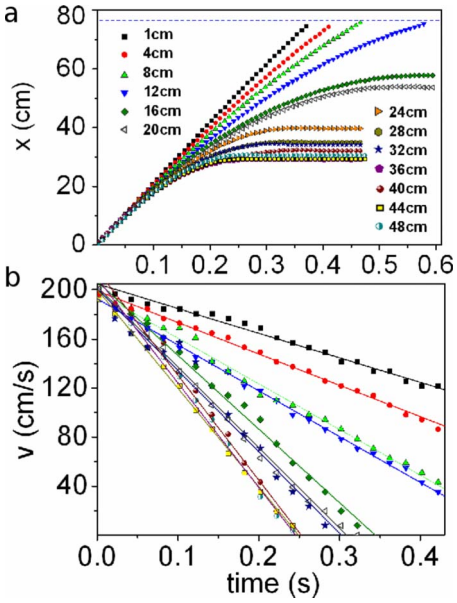

FIG. 2. (Color online) This figure shows the kinematics of the penetrating disk: (a) x vs t and (b) v vs t. The horizontal dotted line in (a) represents the linear field of view, 76 cm; beyond this point the disk disappears from the field of view of the camera. These particular curves, corresponding to different values of h, were obtained with $H=37$ cm and $\rho_i=2.8$ g/cm^3.

intruder has begun to penetrate. The reader will have a clear idea of the experiment by looking at the frontal and lateral views of the movie given as supplementary information [22]. The height h is varied from one monolayer to 48 cm with increments of 4 cm, and five repetitions are made for each height. After each repetition, the material is removed and poured again, in order to start always with the same packing (filling fraction of 0.58). Four intruder densities were considered: 0.7, 1.0, 1.7, and 2.8 g/cm^3. High-speed films permit us to observe the sliding mechanism, verifying that the disk digs through the granular bed sliding on top of its bottom monolayer. The spheres, in contact with the flat surface of the intruder, roll few diameters in the direction of the passing disk. Even if individual spheres are deformable, they are able to collectively support a heavy flat object with negligible deformation. To improve the visualization of the intruder, a bright light-emitting diode (LED) powered by a small and flat battery is put inside the disk pointing toward the base of the container, see Fig. 1(b) and the bottom view of the movie in the supplementary information [22]. We follow the LED spot by a high-speed camera (Lightning RDT Plus) at 500 fps from below and use IMAGEJ to analyze the films. Figures 1(c)–1(e) depict lateral views of the experiment for different heights, where a lump accompanying the disk is observed as it moves inside the bed. Note that the surface of the bed flattens after the passage of the disk. To avoid static charges, the granular bed was treated with anti static spray. All the experiments were made in air [23].

In order to evaluate its full dynamics, we investigated the kinematics of the disk as it moves through the medium. Figure 2(a) depicts the penetration $x(t)$ vs t as h is varied. Figure 2(b) shows the velocities of the intruder measured from the

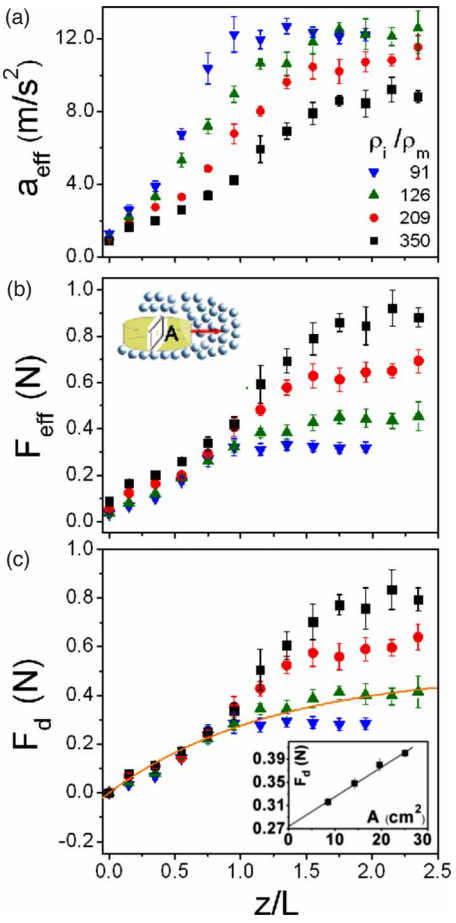

FIG. 3. (Color online) (a) Effective deceleration of the intruder as a function of z/L for different intruder densities. (b) Effective friction forces are calculated by simply multiplying the mass of the intruders by the decelerations plotted in (a). (c) Drag force F_d vs z/L. The sliding friction $ma_{eff}(1)$ has been subtracted to all points. The dotted line is the best fit to the set of points corresponding to $(\rho_i/\rho_m)=126$ using $a(1-e^{-\beta z/L})$, with $a=0.52$ N and $\beta=0.8$. With these values we find that $k=31.4$. The inset shows the linear dependence of the drag force with the cross section of the intruder [shown in the inset of part (b)]. Error bars represent the standard deviation of five events.

tracking trajectories. The fact that they are linear with time means that the curves in Fig. 2(a) can be fitted by the expression $x(t)=V_0t-1/2a_{eff}t^2$, obtaining easily the effective deceleration of the intruder a_{eff}. At $h=h_0$, where $h_0=1$ cm (1 cm of beads guarantees to have always a monolayer underneath the intruder), $x(t)$ is almost a straight line, meaning that the disk travels along the channel with a small deceleration $a_{eff}(h_0)=a_c$. This deceleration is caused by the disk-monolayer contact.

Figure 3(a) shows a_{eff} as a function of z/L, where $L=20$ cm is the width of the channel and z is the depth (the distance from the surface of the bed to h_0, $z=h-h_0$). Each point is the average of five events and each set of points corresponds to a different density.

To find the effective force acting on the intruder, we multiply a_{eff} by its mass [see Fig. 3(b)]. F_{eff} has two contributions: F_c, the friction at the bottom face (disk-monolayer

contact, where the beads are rolling) obtained by multiplying a_c by the mass of the intruder, and F_d, the drag force due to the granular bed acting on the lateral and top faces of the intruder. Figure 3(c) depicts $F_d=F_{eff}-F_c$. We have considered that the contribution of the weight of the particles above the disk to the friction force is negligible, and thus, F_c is constant with z/L. Two interesting behaviors are observed. First, the drag forces collapse for values of $z/L<1$ showing a linear behavior. Second, for larger values of z/L, although the points do not collapse, they saturate. Despite the intruder slides at the bottom of the bed on the first monolayer (and not through a randomly packed granular medium) the first behavior is expected, considering that the intruder is not forced to move inside the bed attached to a vertical rod [21,24]. The second behavior is even more interesting; the saturation of the drag forces observed in Fig. 3(c) suggests a Janssen's effect. As a matter of fact, at $z\sim L$ the weight of the material inside the channel is redirected toward the walls giving rise to a saturated pressure $P(z)=\beta^{-1}\rho_m gL(1-e^{-\beta z/L})$, where β is a constant and $\rho_m=0.58\rho_b$ (ρ_b being the density of the beads). In a first approximation, the drag force may be taken as proportional to the pressure, where the proportionality constant is the effective area $A_{eff}=kA=k\tau d$, see inset of Fig. 3(b). k is a constant that depends only on geometry and on the granularity of the material, independently of the density ratio.

Similarly to $P(z)$ the drag force increases hydrostatically at small heights then it saturates. The only data reasonably well fitted by this expression, however, are the ones corresponding to the lower intruder densities. Due to their larger kinetic energies, the densest intruders fluidize the medium and the drag forces show a delayed saturation.

We also measured the drag force acting on the disk as we vary its thickness τ, keeping its diameter, its mass, and the height of the column (20 cm) constant (being the top area of the disk always the same). A linear dependence with the cross section area is observed [lower inset of Fig. 3(c)]. When A is zero the drag force is only due to the top face-particle contact, which is the major contribution to the drag, explaining the large value of k.

We now focus on the final intruder penetration D as z changes. Figure 4(a) shows D vs z, where similar behaviors are obtained for all the intruder's densities. Each point represents the average of five events. In order to find a suitable expression to model these results, let us analyze what occurs with a given intruder density, for instance, $\rho_i=0.7$ g/cm^3 ($\rho_i/\rho_m=91$). When z is around 4 cm the total penetration of the intruder is 64 cm, and it rapidly diminishes to 10 cm as z increases to 20 cm. Thereafter, D does not decrease further regardless the value of z. A mathematical expression to model this behavior must include then the inverse dependence between D and z together with a saturation effect. Both conditions are obtained if we consider that the impact energy of the intruder is lost by the work done by the drag force [25], i.e., $F_dD=1/2mV_0^2$. Taking $F_d=A_{eff}P(z)$, a simple manipulation of this expression gives the following equation:

$$D=\frac{c\rho_i V_0^2 d}{\rho_m gL}\frac{1}{1-e^{-\beta z/L}}, \tag{1}$$

which can be written as $D'=c(1-e^{-\beta z/L})^{-1}$, where $D'=gL(\rho_m/\rho_i)V_0^{-2}d^{-1}D$ and $c=\beta\pi/8k$. Figure 4(b) shows

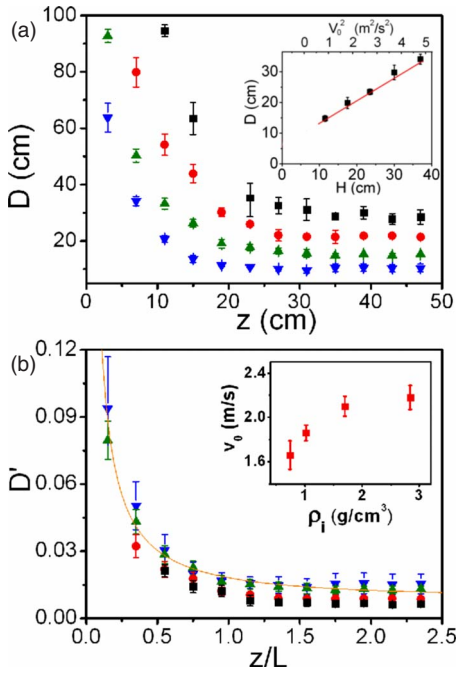

FIG. 4. (Color online) (a) Intruder penetration D as a function of depth z for different intruder densities. All these data were taken using $H=37$ cm. Inset shows a linear dependence of D as a function of H and V_0^2 for $\rho=2.8$ g/cm^3 and $z=23$ cm. The line does not cross the origin because the linear behavior corresponds to the case where the intruder is completely inside the medium. (b) Rescaling D and z by $(\rho_i/\rho_m)V_0^2d(gL)^{-1}$ (see the text), and L respectively, the data collapse reasonably well. The dotted line is the best fit of equation $D'=c(1-e^{-\beta z/L})^{-1}$ to the points corresponding to $(\rho_i/\rho_m)=126$, giving $c=0.01$ and $\beta=0.8$. Inset shows the dependence of V_0 with the intruder density, see the text. For the symbols see Fig. 3.

that with this new variable, coming from the saturation effect of the drag force, the data collapse reasonably well. As a matter of fact, the parameters c and β give the same value of k obtained when fitting F_d in Fig. 3(c). Note that D scales with (ρ_i/ρ_m) instead of $(\rho_i/\rho_m)^{1/2}$ as found in vertical impacts, where gravity is coupled with the drag dynamics. The points corresponding to the larger density ratios are not well fitted with the above parameters. It is clear that the fluidized state, previously invoked to explain the deviation from Janssen's behavior in Fig. 3(c), could explain also this mismatch. It is worth to mention that even at constant H, V_0 changes with ρ_i [inset in Fig. 4(b)]. This is because at larger intruder densities, the energy of the inertial rotation of the beads becomes less significant. Equation (1) suggests, for example, that if the height of the beds were 10 cm our densest intruder would penetrate approximately 3 mm in sand (2.3 g/cm^3) and 7.6 cm in fresh snow (0.1 g/cm^3) compared to the 95 cm in the material studied here.

The photographs shown in Fig. 5 illustrate graphically the singular rheology of the material used in the experiments reported here. A channel is filled with the polystyrene particles and then slowly tilted to find the angle of avalanche [Fig. 5(a)]. Normally, in conventional granular materials made of spherical beads, an intruder buried inside would remain at rest even under avalanche conditions (considering,

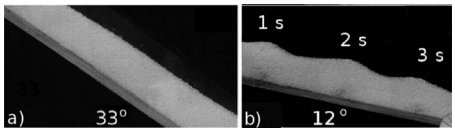

FIG. 5. (a) Angle of avalanche of a bed of polystyrene particles in a tilted channel. (b) Angle of sliding of an intruder inside the bed (see the movie [22]).

of course, that the intruder is buried below the shear band associated with the avalanche). In this superlight material, an intruder with density 2.8 g/cc moves downhill at a small angle without perturbing the bed [see Fig. 5(b) and the movie [22]]. This may indicate that in order to see the same effect in standard granular systems, for example, glass beads, the intruder would be required to have a density of 460 g/cc, well above the density of any known material.

In conclusion, we have studied the dynamics of an intruder moving inside a granular medium with an exceptionally low density. Normally, on denser media the drag forces are very large and impacting intruders stop almost immediately. In the experiments reported here, the intruder penetrates horizontally into a granular medium a long-distance scaling with (ρ_i/ρ_m). As the height of the bed is increased, the shear forces are first hydrostatic and then show a Janssen-like saturation.

This work has been supported by Conacyt, Mexico, under Grant No. 46709.

[1] E. M. Shoemaker, in *Impact and Explosion Cratering*, edited by D. J. Roddy, R. O. Pepin, and R. B. Meril (Pergamon Press, New York, 1977).
[2] H. J. Melosh, *Impact Cratering: A Geologic Process* (Oxford University Press, New York, 1989).
[3] S. T. Thoroddsen and A. Q. Shen, Phys. Fluids **13**, 4 (2001).
[4] M. A. Ambroso, R. D. Kamien, and D. J. Durian, Phys. Rev. E **72**, 041305 (2005).
[5] A. M. Walsh, K. E. Holloway, P. Habdas, and J. R. de Bruyn, Phys. Rev. Lett. **91**, 104301 (2003).
[6] M. P. Ciamarra *et al.*, Phys. Rev. Lett. **92**, 194301 (2004).
[7] J. S. Uehara, M. A. Ambroso, R. P. Ojha, and D. J. Durian, Phys. Rev. Lett. **90**, 194301 (2003).
[8] M. A. Ambroso, C. R. Santore, A. R. Abate, and D. J. Durian, Phys. Rev. E **71**, 051305 (2005).
[9] D. Lohse *et al.*, Phys. Rev. Lett. **93**, 198003 (2004).
[10] D. Lohse, R. Rauhe, R. Bergmann, and D. van der Meer, Nature (London) **432**, 689 (2004).
[11] J. R. Royer *et al.*, Nat. Phys. **1**, 164 (2005).
[12] J. R. Royer, E. I. Corwin, P. J. Eng, and H. M. Jaeger, Phys. Rev. Lett. **99**, 038003 (2007).
[13] H. Katsuragi and D. J. Durian, Nat. Phys. **3**, 420 (2007).
[14] G. Caballero, R. Bergmann, D. van der Meer, A. Prosperetti, and D. Lohse, Phys. Rev. Lett. **99**, 018001 (2007).
[15] A. Seguin, Y. Bertho, and P. Gondret, Phys. Rev. E **78**, 010301(R) (2008).
[16] E. L. Nelson, H. Katsuragi, P. Mayor, and D. J. Durian, Phys. Rev. Lett. **101**, 068001 (2008).
[17] D. J. Costantino *et al.*, Phys. Rev. Lett. **101**, 108001 (2008).
[18] I. Albert *et al.*, Phys. Rev. Lett. **84**, 5122 (2000).
[19] M. E. Cates, J. P. Wittmer, J.-P. Bouchaud, and P. Claudin, Phys. Rev. Lett. **81**, 1841 (1998).
[20] M. B. Stone *et al.*, Nature (London) **427**, 503 (2004).
[21] I. Albert *et al.*, Phys. Rev. E **64**, 061303 (2001).
[22] See EPAPS Document No. E-PLEEE8-80-R12912 for movies of our experiment. The movie shows the frontal, lateral, and bottom views of the sliding intruder. It also shows how an intruder slides down at an angle smaller than the avalanche angle. Finally, it shows two systems with low friction. For more information on EPAPS, see http://www.aip.org/pubservs/epaps.html.
[23] The small velocities of the intruder in this work guarantee that the air-grains interaction is negligible. Indeed, we have carried out several tests in vacuum and found that our results do not change.
[24] R. Albert, M. A. Pfeifer, A. L. Barabási, and P. Schiffer, Phys. Rev. Lett. **82**, 205 (1999).
[25] The contact friction with the monolayer is not taken into account because penetration distances were measured at column heights larger than 4 cm, where drag forces are greater.